



## Supplementary Information for

### **Regulation of cold-induced thermogenesis by the RNA binding protein FAM195A**

Jessica Cannavino<sup>1,2,3</sup>, Mengle Shao<sup>4†</sup>, Yu A. An<sup>4†</sup>, Svetlana Bezprozvannaya<sup>1,2,3</sup>, Shihwei Chen<sup>4</sup>, Jiwoong Kim<sup>5</sup>, Lin Xu<sup>5</sup>, John R. McAnally<sup>1,2,3</sup>, Philipp E. Scherer<sup>4,6</sup>, Ning Liu<sup>1,2,3</sup>, Rana K. Gupta<sup>4</sup>, Rhonda Bassel-Duby<sup>1,2,3</sup>, and Eric N. Olson<sup>1,2,3\*</sup>

\*To whom correspondence should be addressed.

E-mail: [eric.olson@utsouthwestern.edu](mailto:eric.olson@utsouthwestern.edu)

#### **This PDF file includes:**

- Supplementary Methods
- Figures S1 to S4
- Table S1
- Legends for Datasets S1 to S4
- References for SI reference citations

#### **Other supplementary materials for this manuscript include the following:**

- Datasets S1 to S4

## Supplementary Information

### Supplemental Methods

**Chemicals and antibodies.** All chemicals used for cell culture were obtained from Sigma-Aldrich. For Seahorse experiments, palmitate was obtained from Agilent (Agilent 102720) and BCAA were obtained from Sigma Aldrich (Sigma Aldrich; leucine, L8912; isoleucine I7403 and valine V0513) The following antibodies were used in this study: UCP1 antibody 1:1,000 (ab-10983, Abcam), Bckdha antibody 1:1,000 for tissue and 1:500 for cells lysates (ab-90691, Abcam), Cpt2 antibody 1:1,000 (ab-181114, Abcam), Cpt1b antibody 1:1,000 (ab134988, Abcam), OXPHOS cocktail 1:2,000 (ab-110413, Abcam), FAM195A antibody 1:1,000 (MBS2529137, MyBioSource) alpha-tubulin antibody 1:1,000 (T6199, Sigma Aldrich), Tyrosine hydroxylase antibody (ab1542, Millipore-Sigma), GAPDH antibody 1:1,000 (MA15738, Thermo-Fisher), hnRNP/C antibody 2 µg per sample(ab133607, Abcam), TY1 antibody 2µg per sample (Diagenode, C15200054), Goat anti-Mouse IgG 1 (H+L)-HRP Conjugate 1:10,000 (170-6516, Bio-Rad), Goat Anti-Rabbit IgG (H+L)-HRP Conjugate 1:10,000 (170-6515, Bio-Rad), anti-mouse IgG for IP-HRP conjugate antibody 1:5,000 for OXPHOS western blot (ab131368, Abcam) and streptavidin HRP-conjugate antibody 1:1,000 (N100, ThermoFisher).

**Generation of FAM195A KO mice.** KO mice were generated using the clustered regularly interspaced short palindromic repeats (CRISPR)-associated protein 9 (Cas9) gene-editing system by pronuclear and cytoplasmic injection of mouse embryos with Fam195a guide RNA-4 (gRNA-4) and Cas9 mRNA as previously described (1).

The sequence of gRNA-4 (5'- CAC CGA CTC GAT TGA ATA CAA GTC T -3') was

directed against exon 3 of the *Fam195a* gene (also referred to as *MCRIP2*) and cloned into PX458 (PX458 was a gift from Feng Zhang (Addgene plasmid # 48138) (2). Cutting efficiency of gRNA-4 was assessed by T7E1 assay (1), as per provider's instructions (New England BioLabs E3321).

Cas9 mRNA and *Fam195a* gRNAs-4 were injected into the pronucleus and cytoplasm of zygotes and transferred to a surrogate dam for gestation. Mosaic C57BL/6N F0 founders were identified by T7E1 assay on tail biopsies, and positive founders were bred to wild-type C57BL/6N mice to isolate knockout alleles. A founder with a 93-base pair deletion that disrupts the *Fam195a* ORF was chosen to generate the FAM195A KO mouse line. The primers used for genotyping are :

*Fam195a* genotyping -forward: 5'-GCT CTG GTT AAG GAA GGG TCT A -3'

*Fam195a* genotyping -reverse: 5'-CAG AGA GCC AAG GAA AAG TCT -3'

**Body composition measurements.** Live 12-week old male mice were analyzed for total body fat, lean tissue and body water content using an EchoMRI quantitative magnetic resonance system (Echo Medical Systems).

**Acute cold challenge.** In acute cold studies, *ad libitum*-fed 12-week old male mice were transferred from 22°C–23°C to 6°C for five hours. Mice were single-housed without nesting material and food. To monitor temperature, probes (BMDS IPTT UE II, Implantable Electronic ID Transponders) were implanted into the interscapular region of mice and temperature was recorded every hour with a transponder (BMDS IPTT reader, Model: DAS-8007B-IUS). Acute cold studies were started between 9–10 am. Mice were

removed from the cold when their body temperature dropped below 30°C.

**Electromyography.** For monitoring postural muscle EMG, 12-week old male mice were anesthetized and a pair of biopotential leads were placed in contact with the dorsal muscles of the neck. Briefly, an incision was made at the posterior region of the neck to locate the cervical trapezius muscles. The lead wires were then positioned using a 21-gauge needle in approximately 3 mm of muscle tissue perpendicular to the long axis of the fiber bundles. Skin incision was closed using 5-0 suture. After 5 days recovery, mice were used for acute cold exposure experiment. EMG data were collected from the implanted electrodes at a sampling rate of 5 kHz using Ponemach acquisition Software and analysis software.

**Treadmill running.** 12 week-old male mice were run on Exer-3/6 treadmill apparatus (Columbus Instruments) with mild electrical stimulus. The treadmill was set to ramp from 0 to 10 m/min over a period of 5 min and then stay at 10 m/min for an additional 5 min. The treadmill speed then incrementally increased (1 m/min every 5 min) to a maximum speed of 20 m/min until exhaustion. Exhaustion was defined by failure to run for greater than 10 sec.

**Grip strength assay.** Grip strength analysis was performed using a Bioseb Grip Strength Apparatus (BIO-GS3) on 12-week old male mice. The grip strength meter was positioned horizontally while the animal was held by the tail and lowered towards the apparatus. The animal was allowed to grab the metal grid (BIO-GRIPGS) and was

pulled backwards in the horizontal plane. The force applied to the grid immediately before the grip was lost was recorded as the peak tension (grams of force). Each animal performed six pulls for forelimb and hindlimb. The grip strength was represented as the average of the six pulls, divided by the animal body weight.

**Transthoracic echocardiography.** Cardiac function was determined by two-dimensional echocardiography using the Visual Sonics Vevo 2100 Ultrasound (Visual Sonics, Toronto, Ontario, Canada) on conscious 12 week-old WT and FAM195A KO mice. Fractional shortening and ejection fraction were calculated as described previously (3).

**Plasma free amino acids content.** Plasma samples were collected from 12-week old male mice housed at room temperature and after 3 hours of cold exposure. Plasma samples were thawed on ice. One microliter of EDTA free protease inhibitors cocktail was added to 100  $\mu$ L of plasma (1 tablet of cOmplete<sup>TM</sup> EDTA-free protease Inhibitor Cocktail, Cat 5056489001 Millipore-Sigma, Bedford, MA, was dissolved in 1 mL of saline solution). Samples were processed and analyzed in a CLAM 2030 fully automated sample preparation module for LCMS coupled to a Nexera X2 UHPLC system and an LCMS-8060 triple quadrupole mass spectrometer (Shimadzu Scientific Instruments, Columbia, MD). The sample preparation sequence was programmed as follows: addition of 60  $\mu$ L of MeOH onto CLAM 2030 filtration vial; addition of 10  $\mu$ L of sample; addition of 10  $\mu$ L of internal standard cocktail; vortexing during 90 seconds at 1,900 rpm; addition of 50  $\mu$ L of MeOH; vortexing during 60 seconds at 1,900 rpm, filtration during 70 seconds.

Collected sample into the collection vial is then automatically injected for LC/MS/MS analysis (1  $\mu$ L injection). Free amino acids were analyzed using the mass spectrometry parameters and chromatographic conditions described in the Shimadzu LC/MS/MS Method Package for Cell Culture Profiling. The method was edited to include stable isotope labeled free amino acids internal standards SRM transitions.

**Tissue histology and immunostaining.** For H&E staining, mouse tissues were fixed in 4% formalin overnight at RT. Tissues were dehydrated and embedded in paraffin for routine histological analyses and staining for hematoxylin and eosin, as previously described (4). For immunofluorescence, BAT was dissected, flash-frozen in a cryoprotective tissue-freezing medium (Triangle BioSciences International) and sectioned on a cryostat. Subsequentially, slices (30  $\mu$ m) were stained with tyrosine hydroxylase antibody as previously described (5).

**SVF differentiation.** Differentiation into brown adipocytes was induced by treating confluent SVF cultures with an induction media (high-glucose DMEM media supplemented with 10% FBS, 20 mM HEPES [pH 7.4], 10 nM T3, 0.1 mg ml<sup>-1</sup> insulin, 1  $\mu$ M dexamethasone, 0.5 mM isobutylmethoxyxanthine and 0.125 mM indomethacin) for 48 hr. Two days after induction, the cells were kept in maintenance media (high-glucose DMEM media supplemented with 10% FBS, 20 mM HEPES [pH 7.4], 10 nM T3, and 0.1 mg ml<sup>-1</sup> insulin) for 5-7 days.

For SVF differentiation into white adipocytes, confluent cultures were treated with white adipogenic cocktail (DMEM supplemented with 5  $\mu$ g ml<sup>-1</sup> insulin, 1  $\mu$ M

dexamethasone, and 0.5 mM isobutylmethoxyxanthine) for 48 hr. After 48 hr cells were maintained in growth media supplemented with 5  $\mu\text{g ml}^{-1}$  insulin and cultured in the presence or absence of 1  $\mu\text{M}$  rosiglitazone.

**Lentivirus infection.** Lenti-X cell (Takara Bio) were transfected with 6.2  $\mu\text{g}$  of PAX2, 2.0  $\mu\text{g}$  of pMD2 and 8.3  $\mu\text{g}$  of shRNAs using FuGENE 6. After 48 h of transfection, supernatants were collected and filtered through a 0.45  $\mu\text{m}$  syringe filter. Viruses were concentrated with Lenti-X concentrator (631232, Takara) for 16 h at 4°C. After centrifugation at 1,500g for 45 min viral pellet was resuspended in Optimem media (31985070, Gibco). Concentrated viral soups were then diluted 1:50 into SVF growth medium supplemented with polybrene at the final concentration of 8  $\mu\text{g/ml}$ . After 48 h of infection, infected cells were selected by replacing viral media with fresh growth media supplemented with 5  $\mu\text{g/ml}$  puromycin.

**DNA constructs for over expression and knock down studies.** The open reading frame (ORF) for FAM195A was obtained in pCMV-SPORT-6 backbone (MMM1013-202767770, Horizon). FAM195A ORF was subcloned into the following custom-made pMXs-puro (RTV-012, Cell Biolabs) backbones: pMXs-puro-TY1 (N-terminal) and pMXs-puro-miniTurbo (C-terminal). pMXs-puro-miniTurbo was generated by conventional cloning (7) using pcDNA-V5-miniTurbo-NES (pcDNA-V5-miniTurbo-NES was a gift from Alice Ting Addgene plasmid # 107170) as the PCR template (8). The open reading frame of human Znf281, JunB, Fip1L1 and Safb was obtained from Gateway-compatible human ORF library, purchased from ThermoFisher Scientific. JunB, Fip1L1 and Safb ORFs were

cloned into pMH-Flag-HA construct (9) by performing site-specific LR recombination using Gateway LR Clonase II enzyme mix kit (ThermoFisher Scientific) (pMH-Flag-HA was a gift from Michael Huen Addgene plasmid # 101766). Znf281 ORF was cloned into custom-made pMXs-FLAG as previously described (10). For knock down studies pre-cloned shRNA constructs were purchased from Sigma (Sigma- Aldrich MISSION® shRNA).

**Sodium arsenite treatment and immunofluorescence.** To induce RNA stress granule, differentiated brown adipocytes were treated with 500  $\mu$ M sodium arsenite in maintenance medium for 1 h at 37°C in the cell culture incubator. Adipocytes treated with DMSO were used as control. Upon treatment, cells were fixed in 4% PFA for 10 min and subsequently stained with FAM195A antibody (1:200) overnight at 4°C as previously described (11). Fluorescence microscopy of fixed cells was carried out using a Zeiss LSM-800 confocal microscope.

**Labeling of FAM195A-associated RNA.** SVF cells stably expressing TY1-FAM195A were differentiated into brown adipocytes. After differentiation cells were washed twice with PBS and irradiated with UV light at 254 nm (150 mJ/cm<sup>2</sup>) on ice. Immediately after irradiation, cells were lysed, and lysates were incubated with low or high concentration (1:500 or 1:50) of RNase I (Ambion) for 3 min at 37°C. TY1 fusion proteins and hnRNP/C proteins were captured by incubation with the TY1 antibody (Diagenode) or hnRNP/C antibody (Abcam) and 100  $\mu$ l Dynabeads overnight at 4°C. Cross-linked RNA–protein complexes were labelled and visualized as previously described (11).



**Oxygen consumption assay.** *Ex vivo* mitochondrial respiration of noradrenaline-induced respiration in presence of BCAAs and palmitate were determined using the Seahorse XF24 Extracellular Flux Analyzer (Agilent, Santa Clara, CA, USA). BAT fat pads from 12-week old male animals (1.5–3.5 mg) were maintained in KRB-HEPES buffer (15 mM glucose, 200 mM adenosine, and 2% BSA). During OCR measurements, tissues were incubated with 3 mM BCAA and subsequently stimulated with noradrenaline (2  $\mu$ M) at the indicated time point.

**Complex I activity.** For Complex I activity frozen BAT powders were lysed using ice cold PBS plus protease inhibitor and homogenized for 25 strokes with a dounce homogenizer. Complex I activity was detected according to manufacture protocol (ab10972, Abcam).

**Relative quantitation of proteins using Tandem Mass Tags (TMT) and Mass Spectrometry (MS).** Protein concentration was determined by BCA assay (23225, ThermoFisher) and 25  $\mu$ g of protein were processed by UTSW proteomic core. Briefly, samples were suspended in 5% SDS with 50mM triethylammonium bicarbonate (TEAB). DTT was added to a final concentration of 10 mM and samples were incubated at 56°C for 30 min. After cooling, iodoacetamide was added to a final concentration of 20 mM and samples were incubated for 30 min at room temperature in dark. Following centrifugation for 2 min at 13.2k rpm, the supernatants were removed, of which 50  $\mu$ L of each were digested overnight with trypsin at 37°C using an S-Trap (Protifi). Following digestion, the peptide eluate was dried and reconstituted in 100 mM TEAB buffer. The samples were

labelled with TMT reagent, quenched with 5% hydroxylamine, and combined. A reverse-phase fractionation spin column (Pierce) was used according to the manufacturer's directions to fractionate the sample into 8 fractions. The fractions were dried in a SpeedVac and reconstituted in a 2% acetonitrile, 0.1% TFA buffer. Fractions were injected onto an Orbitrap Fusion Lumos mass spectrometer coupled to an Ultimate 3000 RSLC-Nano liquid chromatography system. Samples were injected onto a 75  $\mu\text{m}$  i.d., 75-cm long EasySpray column (Thermo) and eluted with a gradient from 0-28% buffer B over 180 min. Buffer A contained 2% (v/v) ACN and 0.1% formic acid in water, and buffer B contained 80% (v/v) ACN, 10% (v/v) trifluoroethanol, and 0.1% formic acid in water. The mass spectrometer operated in positive ion mode with a source voltage of 1.6 kV and an ion transfer tube temperature of 275 °C. MS scans were acquired at 120,000 resolution in the Orbitrap and top speed mode was used for SPS-MS3 analysis with a cycle time of 2.5 sec. MS2 was performed with CID with a collision energy of 35%. The top 10 fragments were selected for MS3 fragmentation using HCD, with a collision energy of 55%. Dynamic exclusion was set for 25 s after an ion was selected for fragmentation. Raw MS data files were analyzed using Proteome Discoverer v2.2 (Thermo), with peptide identification performed using Sequest HT searching against the mouse protein database from UniProt. Fragment and precursor tolerances of 10 ppm and 0.6 Da were specified, and three missed cleavages were allowed. Carbamidomethylation of Cys and TMT labelling of N-termini and Lys side-chains were set as a fixed modification, with oxidation of Met set as a variable modification. The false-discovery rate (FDR) cutoff was 1% for all peptides. Protein abundances were normalized based on the total abundance in each sample. Protein with 1Log<sub>2</sub>-fold or greater in WT respect to KO and *P* value<0.05 were

considered for Gene Ontology analysis and STRING network analysis.

STRING network analysis was performed by using the following parameters. Active interaction sources: textmining, experiments, databases, co-expression, and co-occurrence. The interaction score was set to high confidence

**RNA sequencing.** RNA-seq was performed by the UT Southwestern Genomic and Microarray Core Facility.

Briefly, Trim Galore ([https://www.bioinformatics.babraham.ac.uk/projects/trim\\_galore/](https://www.bioinformatics.babraham.ac.uk/projects/trim_galore/)) was used for quality and adapter trimming. The mouse reference genome sequence and gene annotation data, mm10, were downloaded from Illumina iGenomes ([https://support.illumina.com/sequencing/sequencing\\_software/igenome.html](https://support.illumina.com/sequencing/sequencing_software/igenome.html)). The qualities of RNA-sequencing libraries were estimated by mapping the reads onto mouse transcript and ribosomal RNA sequences (Ensembl release 89) using Bowtie (v2.3.4.3) (Langmead and Salzberg, 2012). STAR (v2.7.2b) (12) was employed to align the reads onto the mouse genome, SAMtools (v1.9) (13) was employed to sort the alignments, and HTSeq Python package(14) was employed to count reads per gene. edgeR R Bioconductor package(15) was used to normalize read counts and identify differentially expressed (DE) genes. Gene ontology (GO) data was downloaded from NCBI FTP (<ftp://ftp.ncbi.nlm.nih.gov/gene/DATA/gene2go.gz>). The enrichment of DE genes to pathways and GOs were calculated by Fisher's exact test in R statistical package. Differentially expressed genes were determined using cut-offs of fold changes > 1.5 and FDR-adjusted p-value < 0.05. RT-PCR primers used are indicated in Table S1

**ChIP sequencing data analysis.** Published ChIP-seq data were downloaded from GEO under accession number accession code GSE43763 (<https://www.ncbi.nlm.nih.gov/geo/query/acc.cgi?acc=GSE43763>) and GSE97116 (<https://www.ncbi.nlm.nih.gov/geo/query/acc.cgi?acc=GSE97116>). Paired-end raw reads were mapped to the mouse reference genome (GRCh38/mm10) using bowtie2 (version 2.3.4.3) with parameter ‘–very-sensitive’ enabled. Read duplication and reads that mapped to chrM were removed from downstream analysis. Peaks were called using findpeaks command from HOMER software package version 4.9, with parameter ‘–style dnase’, and the FDR threshold (for Poisson p-value cutoff) was set to 0.001.

**Proximity biotinylation and protein identification by mass spectrometry.** Proximity biotinylation (BioID) was adapted from prior publications (8). Two independent BioID experiments were performed. Briefly, after 7 days of differentiation of SVF cells stably expressing pMXs-puro-FAM195A-miniTurbo, ten 15 cm dishes containing mature adipocytes were obtained. Five 15 cm dishes were supplemented with 50  $\mu$ M biotin (B4501, Sigma) in adipocytes maintenance media for 2 h. To wash excess of biotin cells were then incubated with fresh media without biotin for 45 min (BIO+). The remaining five 15 cm dishes were used as negative control and were left untreated (BIO-). Cell lysates were extracted in 1 ml of lysis buffer (RIPA lysis buffer, 6 M urea, supplemented with cOmplete protease inhibitor cocktail and PhosSTOP phosphatase inhibitor cocktail) and mechanically lysed with a 27-gauge syringe. Lysates were added to 9 ml of dilution buffer (50 mM Tris, 150 mM NaCl) and 100 $\mu$ l of equilibrated streptavidin magnetic beads (88816, ThermoFisher). Lysates were incubated O/N at 4°C on a wheel. Beads were

washed 5 times with lysis buffer and boiled for 5min in 2x Laemmli sample buffer (1610737, Bio-Rad). For protein identification by mass spectrometry, samples were run for 1 cm in an Any-KD Mini-PROTEAN 10-well gel (4569034, Bio-Rad). Gels were then fixed and stained with EZBlue (G1041, Sigma) as per provider's instructions. The area of the gel containing proteins was cut into small 1 mm cubes and submitted for analysis to the Proteomics Core Facility at University of Texas Southwestern Medical Center. Gel band samples were digested overnight with trypsin (Pierce) following reduction and alkylation with DTT and iodoacetamide (Sigma). The samples then underwent solid-phase extraction cleanup with an Oasis HLB plate (Waters) and the resulting samples were injected onto an Orbitrap Fusion Lumos mass spectrometer coupled to an Ultimate 3000 RSLC-Nano liquid chromatography system. Samples were injected onto a 75  $\mu$ m i.d., 75-cm long EasySpray column (ThermoFisher) and eluted with a gradient from 0-28% buffer B over 90 min. Buffer A contained 2% (v/v) ACN and 0.1% formic acid in water, and buffer B contained 80% (v/v) ACN, 10% (v/v) trifluoroethanol, and 0.1% formic acid in water. The mass spectrometer operated in positive ion mode with a source voltage of 1.8 kV and an ion transfer tube temperature of 275°C. MS scans were acquired at 120,000 resolution in the Orbitrap and up to 10 MS/MS spectra were obtained in the ion trap for each full spectrum acquired using higher-energy collisional dissociation (HCD) for ions with charges 2-7. Dynamic exclusion was set for 25 sec after an ion was selected for fragmentation.

Raw MS data files were analyzed using Proteome Discoverer v2.2 (ThermoFisher), with peptide identification performed using Sequest HT searching against the mouse protein database from UniProt. Fragment and precursor tolerances of

10 ppm and 0.6 Da were specified, and three missed cleavages were allowed. Carbamidomethylation of Cys was set as a fixed modification, with oxidation of Met set as a variable modification. The false-discovery rate (FDR) cutoff was 1% for all peptides. Protein abundance values were calculated by normalizing the protein abundances obtained from cells pulsed with biotin (BIO+) to the abundance of the same protein purified in un-pulsed cells (BIO-). Protein hits were obtained by filtering results from both experiments (>20-fold enrichment in “Biotin” samples to “Control” samples) and were used for analysis on GO and STRING network analysis.

STRING network analysis was performed by using the following parameters. Active interaction sources: textmining, experiments, databases, co-expression, and co-occurrence. The interaction score was set to medium confidence

In order to validate the hits obtained with BioID experiments performed, SVF cells were stably infected with pMXs-puro-FAM195A-miniTurbo and pMH-Flag-Fip1L1, pMH-Flag-Safb, pMH-Flag-JunB and pMXs-puro-Flag-Znf281. Two 10 cm dishes were pulsed with biotin while other two 10 cm dishes were left untreated. Immunoprecipitated proteins were analyzed by standard western blot analysis.

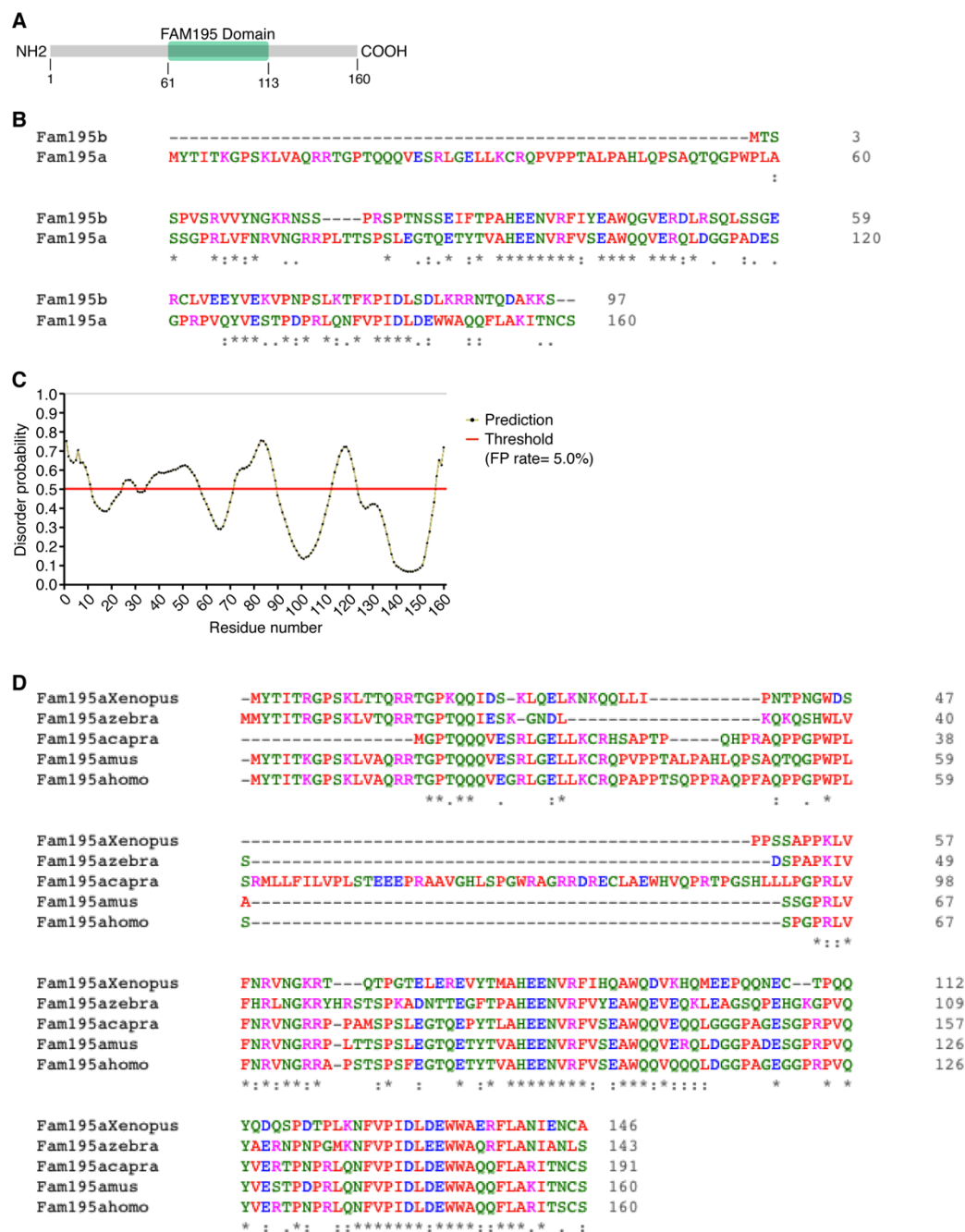


**Fig. S1. FAM195A protein conservation.**

(A) Model of FAM195A protein prediction based on NCBI conserved domain database (CDD). According to the model, FAM195A protein contains a FAM195 domain spanning from amino acid 61 to 113.

(B) Amino acid sequence alignment of *Mus musculus* FAM195A with FAM195B protein.

(C) FAM195A disordered domains spanning amino acid 1 to 10, 25 to 29, 35 to 56, 72 to 89, 113 to 123 and 157 to 160. FP rate; false positive rate (Protein DisOrder prediction System, PrDOS).

(D) Amino acid sequence alignment of vertebrate FAM195A proteins. Colors of amino acid residues indicate their properties (pink, positive charge; blue, negative charge; red, hydrophobic; green, hydrophilic). The symbols below the alignment represent the biochemical similarity of aligned amino acids with asterisks indicating identity, colons representing high similarity, and periods showing somewhat similar conservation.



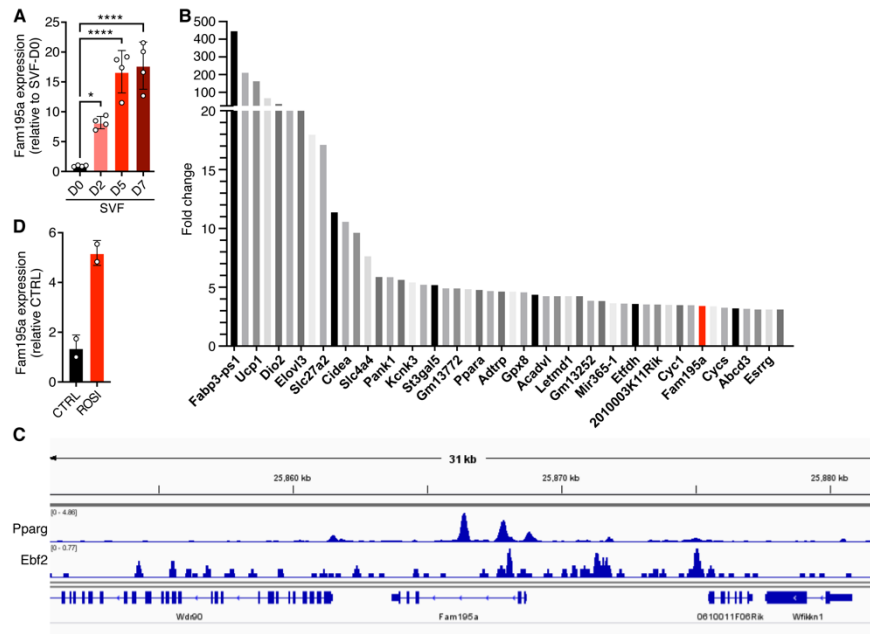


**Fig. S2. FAM195A protein regulation.**

(A) qRT-PCR showing Fam195a expression during adipogenic differentiation of immortalized SVF fibroblasts obtained from BAT. \*  $P$  value < 0.05, and \*\*\*\* $P$  value < 0.0001.

(B) Microarray analysis showing the top 50 genes significantly upregulated in iWAT of Zfp423KO mice. Fam195a is indicated with a red bar ( $P$  value= 0.025).

(C) Ebf2 and Pparg ChIP-seq profiles for the *Fam195a* gene locus.

(D) qRT-PCR showing Fam195a expression in adipogenic differentiated iWAT-derived SVF fibroblasts treated with rosiglitazone (ROSI) or DMSO (CTRL).

Data are shown as mean  $\pm$  STD; one way ANOVA (A).

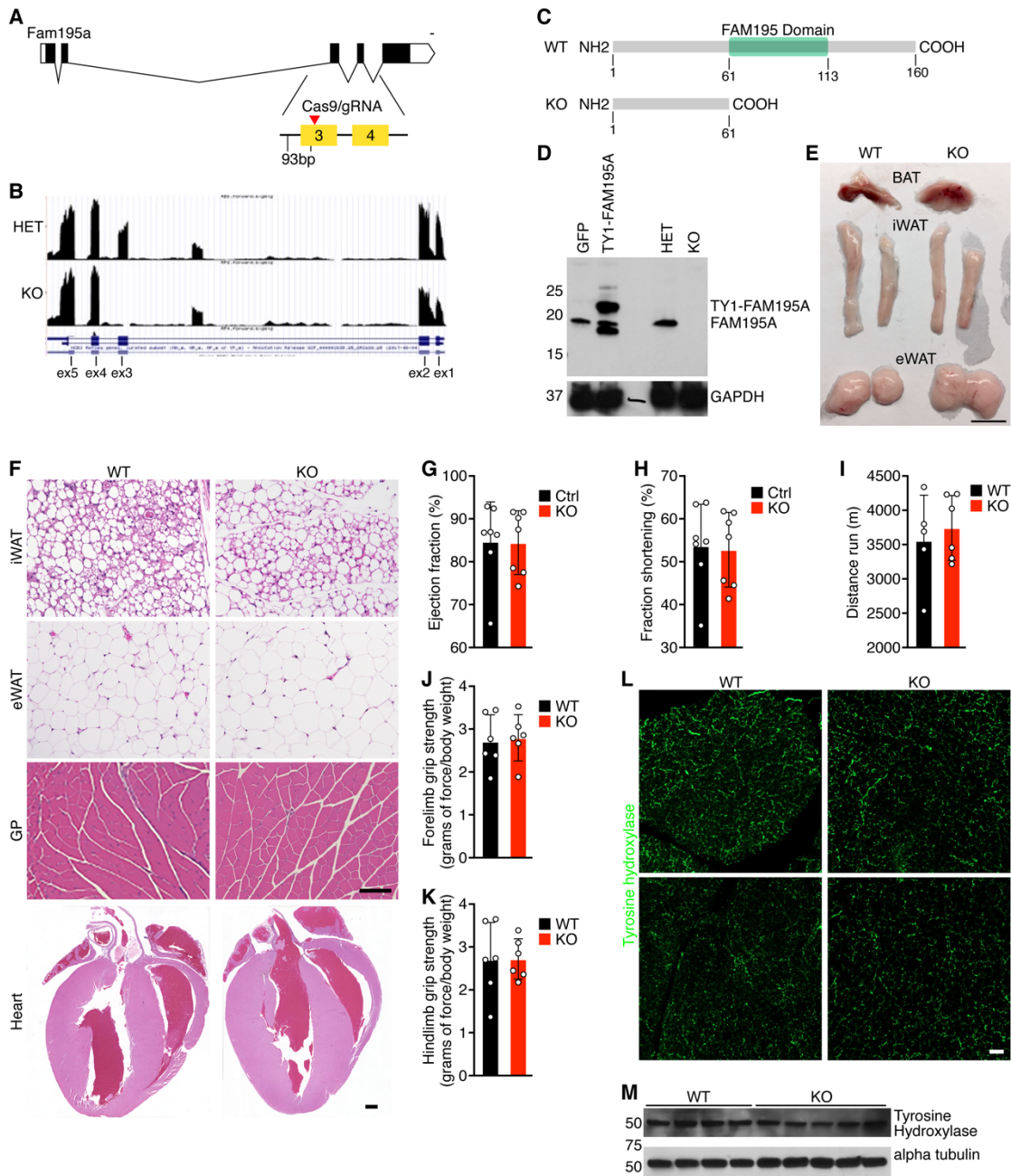


**Fig. S3. Generation and phenotyping of FAM195A KO mice.**

(A) A deletion of 93 bp from within intron 2 into exon 3 of the *Fam195a* gene was generated using the CRISPR-Cas9 system.

(B) Representative RNA-seq tracks from HET and KO FAM195A mice. Tracks show skipping of exon 3 in FAM195A KO BAT.

(C) Schematic illustration of FAM195A proteins.

(D) Western blot analysis showing FAM195A expression in HET and KO mice. Myotubes expressing GFP and TY1-FAM195A were used as a control for antibody specificity. GAPDH was used as a loading control.

(E) Representative photographs showing BAT, iWAT and eWAT dissected from WT and FAM195A KO mice. Scale bar, 1cm.

(F) Representative H&E staining of iWAT, eWAT, GP and heart from WT and FAM195A KO mice. Scale bar, 50  $\mu$ m for iWAT, eWAT and GP; Scale bar, 500  $\mu$ m for heart.

(G and H) Cardiac function of WT and FAM195A KO heart. n=7 for 12-week-old male mice.

(I) Treadmill exhaustion running. n=5-6 for 12-week-old male mice for each genotype.

(J) Forelimb grip strength test. n=6 for 12-week-old male mice for each genotype.

(K) Hindlimb grip strength test. n=6 for 12-week-old male mice for each genotype.

(L) Tyrosine hydroxylase (green) immunofluorescence staining of BAT from two WT and two FAM195A KO mice. Scale bar, 50 $\mu$ M.

(M) Western blot analysis showing tyrosine hydroxylase expression in WT and FAM195A KO BAT. Alpha-tubulin was used as a loading control. Data are shown as mean  $\pm$  STD. BAT, interscapular brown adipose tissue; iWAT, inguinal white adipose tissue; eWAT epididymal white adipose tissue; GP, gastrocnemius plantaris.



**Fig. S4. Gene expression profile of FAM195A KO BAT.**

(A) Top enriched gene ontology terms relative to proteins down-regulated in Fig. 4A.

(B) Heatmap showing log<sub>2</sub> (fold change (FC)) of genes regulated in BAT of FAM195A KO and HET mice.

(C) Gene ontology molecular mechanism analysis top enriched terms for down-regulated genes in (B).

(D) Gene ontology cellular component analysis top enriched terms for downregulated genes in (B).

(E) GeneMANIA analysis. Proteins with similar expression profile of FAM195A are connected with a pink line. Proteins with the FAM195 domain are connected with a green line. Proteins predicted to interact with FAM195A are connected with an orange line. Asterisks indicate proteins that are significantly down-regulated in the FAM195A KO BAT proteome.

(F) Diagram indicating enzymes responsible for BCAA leucine oxidation to Acetyl-CoA. For each enzyme the log<sub>2</sub>FC down-regulation in FAM195A KO BAT proteome is indicated.

(G and H) qRT-PCR of selected genes identified in (B) comparing WT and FAM195A KO mice. qRT-PCR analysis was performed for genes associated with BCAA metabolism (G) and mitochondria respiration (Cox15 and Etf<sub>dh</sub>) and fatty acid transport (Cpt2 and Cpt1b) (H). \*\* *P* value < 0.01, \*\*\* *P* value < 0.001 and \*\*\*\**P* value < 0.0001.

Data are presented as mean ± SD (G,H); unpaired *t*-test (G,H).

**Table S1.** List of primers used.

Gene	Forward 5'-3'	Reverse 5'-3'
<i>Bckdha</i>	AGGAGGTGCTGAAGTTCTACC	CGCCATAGTTGGTCATGTAGAAG
<i>Bcat2</i>	TTCCAGAACCTCACGCTACAC	TAGCAGAACGTAGCATCCTGTC
<i>Mccc1</i>	TGACGTATAACCGCGATGGG	GGAAAGATCGCCCAGGACTC
<i>Mccc2</i>	GAGTGTCTGGGGGTAGAATGC	TAAGTTGGCCCCCTCCTGAGT
<i>Ivd</i>	GTATTGATGAGCGGGCTGGA	GACGTA CTGTCTGACTTGCCA
<i>Acat1</i>	CTGGGCGCAGGTTTACCTAT	GGTGTTGCTCCTCTGCTCAT
<i>Cox15</i>	CAACGGTTGCTCCTTCCGTC	GTCCCTTTTCCGGATTGCAG
<i>Etfdh</i>	TGGCCCTTGGACAGACATAC	CGGAATGGACTCAGGTACGG
<i>Cpt2</i>	GACTATTCGCCAGCTTCCA	GCTGCCAGATACCGTAGAGC
<i>Fam195a</i>	ATCCCCGGCTACAGA ACTTT	CAACAGGTGCAAAAAGTCCAA
<i>Ucp1</i>	TCTCAGCCGGCTTAATGACTG	GGCTTGCATTCTGACCTTCAC
<i>Prdm16</i>	ACACGCCAGTTCTCCAACCTGT	TGCTTGTTGAGGGAGGAGGTA
<i>Pgc1a</i>	GCACCAGAAAACAGCTCCAAG	CGTCAAACACAGCTTGACAGC
<i>Dio2</i>	CATTGATGAGGCTCACCCCTTC	GGTTCCGGTGCTTCTTAACCT
<i>Cox8b</i>	TGCTGGAACCATGAAGCCAAC	AGCCAGCCAAA ACTCCC ACTT
<i>Cpt1b</i>	ACTAACTATGTGAGTGACTGG	TGGCATAATAGTTGCTGTTT
<i>Klf15</i>	AAAATAGTAGCTCCCAGAGG	CTATGGCTCCATTTGTCTTG
<i>Esrra</i>	CTTAATCCGATCTCTCCTCTCC	CTGCTTGGATTATTGCTTC
<i>Ppara</i>	GATGTCACACAATGCAATTC	CAGTTTCCGAACAAGGTC
<i>Rps18</i>	CATGCAAACCCACGACAGTA	CCTCACGCAGCTTGTTGTCTA
<i>18S</i>	ACCGCAGCTAGGAATAATGGA	GCCTCAGTTCCGAAAACCA

**Dataset S1.** Numerical data to support Fig. 3A.

**Dataset S2.** Abundance of proteins identified in Fig. 4A.

**Dataset S3.** Numerical data supporting Fig. 4E.

**Dataset S4.** Abundance of proteins identified in Fig. 6C.

## References

1. C. Long *et al.*, Prevention of muscular dystrophy in mice by CRISPR/Cas9-mediated editing of germline DNA. *Science* **345**, 1184-1188 (2014).
2. F. A. Ran *et al.*, Genome engineering using the CRISPR-Cas9 system. *Nat Protoc* **8**, 2281-2308 (2013).
3. C. A. Makarewich *et al.*, The DWORF micropeptide enhances contractility and prevents heart failure in a mouse model of dilated cardiomyopathy. *Elife* **7** (2018).
4. J. M. Shelton, M. H. Lee, J. A. Richardson, S. B. Patel, Microsomal triglyceride transfer protein expression during mouse development. *J Lipid Res* **41**, 532-537 (2000).
5. X. Zeng *et al.*, Innervation of thermogenic adipose tissue via a calsyntenin 3beta-S100b axis. *Nature* **569**, 229-235 (2019).
6. M. Shao *et al.*, Zfp423 Maintains White Adipocyte Identity through Suppression of the Beige Cell Thermogenic Gene Program. *Cell Metab* **23**, 1167-1184 (2016).
7. A. Ramirez-Martinez *et al.*, The nuclear envelope protein Net39 is essential for muscle nuclear integrity and chromatin organization. *Nat Commun* **12**, 690 (2021).
8. T. C. Branon *et al.*, Efficient proximity labeling in living cells and organisms with TurboID. *Nat Biotechnol* **36**, 880-887 (2018).
9. L. An *et al.*, Dual-utility NLS drives RNF169-dependent DNA damage responses. *Proc Natl Acad Sci U S A* **114**, E2872-E2881 (2017).
10. H. Zhou *et al.*, ZNF281 enhances cardiac reprogramming by modulating cardiac and inflammatory gene expression. *Genes Dev* **31**, 1770-1783 (2017).
11. D. M. Anderson *et al.*, Severe muscle wasting and denervation in mice lacking the RNA-binding protein ZFP106. *Proc Natl Acad Sci U S A* **113**, E4494-4503 (2016).
12. A. Dobin *et al.*, STAR: ultrafast universal RNA-seq aligner. *Bioinformatics* **29**, 15-21 (2013).
13. H. Li *et al.*, The Sequence Alignment/Map format and SAMtools. *Bioinformatics* **25**, 2078-2079 (2009).
14. S. Anders, P. T. Pyl, W. Huber, HTSeq--a Python framework to work with high-throughput sequencing data. *Bioinformatics* **31**, 166-169 (2015).
15. R. C. Gentleman *et al.*, Bioconductor: open software development for computational biology and bioinformatics. *Genome Biol* **5**, R80 (2004).

